Behavior near $\theta = \pi$ of the mass gap in the two-dimensional O(3) nonlinear sigma model

B. Allés,[1,*] M. Giordano,[2,†] and A. Papa[3,‡]

[1]*INFN Sezione di Pisa, Largo Pontecorvo 3, 56127 Pisa, Italy*

[2]*Institute for Nuclear Research of the Hungarian Academy of Sciences (ATOMKI), Bem tér 18/c, H-4026 Debrecen, Hungary*

[3]*Dipartimento di Fisica, Università della Calabria and INFN Gruppo Collegato di Cosenza, Arcavacata di Rende, 87036 Cosenza, Italy*

The validity of Haldane's conjecture entails that the mass gap of the two-dimensional O(3) nonlinear sigma model with a θ term must tend to zero as θ approaches the value π by following a precise law. In the present paper we extract the related critical exponents by simulating the model at imaginary θ.

I. INTRODUCTION

The proposal of Haldane in Refs. [1–3], regarding the absence of a gap in the spectrum of one-dimensional (1D) (throughout the paper nD means n-dimensional) quantum chains of half-integer spins interacting through an antiferromagnetic coupling, prompted a great deal of work aimed at checking its correctness. Apart from numerical simulations and direct analytical scrutiny on such 1D quantum chains [4–9], an important step towards the clarification of the validity of this proposal was achieved by demonstrating that such chains and the 2D O(3)-invariant nonlinear sigma model with a topological term at vacuum angle $\theta = \pi$ share the same long-distance behavior; see Refs. [1,2,10,11]. Hence the above property can also be verified by studying the 2D O(3) nonlinear sigma model near $\theta = \pi$. Although direct Monte Carlo simulations are currently unfeasible for $\theta \neq 0$ due to the sign problem[1] [see (3) below], several tricks have been contrived to analyze the model at nonzero θ and, particularly, at $\theta = \pi$. They are as follows: (i) in Refs. [13–15] the distribution of the topological charge was determined at $\theta = 0$ and then used to reweight the partition function at $\theta \neq 0$; (ii) in Ref. [16] the mass gap was extracted as a function of imaginary θ [with which the sign problem disappears; see (3) below] and the results extrapolated to real θ; (iii) in Refs. [17,18] a similar method was employed, measuring the expectation value of the topological charge at imaginary θ, after which a controlled way to perform the extrapolation allowed the authors to reduce the uncertainties. In all cases a decisive confirmation of Haldane's conjecture, namely, the mass gap of the 2D O(3) nonlinear sigma model vanishes at $\theta = \pi$, was obtained.

The equivalence between 1D antiferromagnetic chains of spins and the 2D O(3) nonlinear sigma model with $\theta = \pi$ has been further investigated. It was argued in Refs. [19,20] that the critical theory for the half-integer quantum antiferromagnetic spin chains is the Wess-Zumino-Novikov-Witten (WZNW) model with

a topological coupling $k = 1$, defined in Refs. [21–23]. This model is the stable fixed point of the 2D O(3) nonlinear sigma model with a vacuum angle $\theta = \pi$. The renormalization group considerations of Refs. [19,20] on the WZNW model lead to the conclusion that the mass gap of the 2D O(3) nonlinear sigma model tends to zero while approaching $\theta = \pi$ from below as

$$m(\theta) \propto (\pi - \theta)^{\epsilon_{\text{WZNW}}} \left(\log \frac{1}{\pi - \theta} \right)^{-\beta_{\text{WZNW}}}, \qquad (1)$$

for $0 < \pi - \theta \ll 1$. The WZNW predictions are $\epsilon_{\text{WZNW}} \equiv \frac{2}{3}$ and $\beta_{\text{WZNW}} \equiv \frac{1}{2}$. Therefore, another type of useful check of Haldane's conjecture consists in finding the critical exponents in (1) from numerical simulations of the 2D O(3) nonlinear sigma model with a nonzero θ term. In Refs. [13–15] the authors compared the numerical results with the theoretical prediction for the step scaling function, finding good agreement. In this paper we want to approach this issue in a different way, attempting instead at a determination of both the critical exponent and the exponent of the logarithmic correction, from Monte Carlo simulations at imaginary θ using the method of Ref. [16] together with the improvement procedure of Refs. [17,18].[2] A similar approach was used in Ref. [18], where however the theoretical expectation for the logarithmic term was used as an input in the analysis. As we shall see along the present paper, a direct detection of the power of the logarithmic correction in Eq. (1) requires an extremely accurate control of the statistics and error bars, an endeavor that seems to lie beyond present-day capabilities. It is however possible to bypass this difficulty, by combining the analyses of the mass gap and of the topological charge. The purpose of our paper consists precisely in employing this combined analysis to retrieve the exponents ϵ_{WZNW} and β_{WZNW} in Eq. (1).

In Sec. II the 2D O(3) nonlinear sigma model with a θ term is introduced and its main properties briefly enumerated. In Sec. III the Monte Carlo method and related difficulties shall be presented. In Sec. IV the basics of the extrapolation method from imaginary to real θ will be explained, while the difficulties related to the presence of logarithmic corrections in Eq. (1) are attacked in Secs. V and VI. In Sec. VI also the

_____

*alles@df.unipi.it

†giordano@atomki.mta.hu

‡papa@fis.unical.it

[1]Nevertheless, an effort has recently been pursued to avoid the sign problem by simulating the model at $\theta \neq 0$ after demonstrating the equivalence of its continuum limit with that of the dual of the SU(2) principal chiral model with a fixed radial part; see Ref. [12].

_____

[2]As it was apparent in Ref. [16], the results of the simulations for the mass gap alone are too noisy to allow a reasonably clear determination of the exponents in Eq. (1).

details of the data analysis will be spelled out. The conclusions are listed in Sec. VII.

II. 2D O(3) NONLINEAR SIGMA MODEL

The action of the 2D O(3) nonlinear sigma model with a θ term in the continuum is given by

$$S = A - i\theta Q, \quad A = \frac{1}{2g} \int d^2x (\partial_\mu \vec{\phi}(x))^2,$$

$$Q = \int d^2x \, Q(x), \tag{2}$$

$$Q(x) \equiv \frac{1}{8\pi} \epsilon^{\mu\nu} \epsilon_{abc} \phi^a(x) \partial_\mu \phi^b(x) \partial_\nu \phi^c(x),$$

where g is the coupling constant, θ the vacuum angle, $Q(x)$ the topological charge density, and Q the total topological charge. $\vec{\phi}(x)$ is a three-component unit vector that represents a classical spin, the dynamical variable at position x. The renormalized Q takes on integer values because it counts how many times the spin variables wrap around the unit sphere.

This model enjoys various properties that make it an interesting object of study in areas ranging from condensed matter to field theory. In particular, the quantum Hall effect can be studied by it (see, for example, Ref. [24]) and some attributes of field theories like asymptotic freedom, spontaneous generation of a gap, or instantonic effects are present in the 2D O(3) nonlinear sigma model; see Ref. [25]. Specifically, the mass gap at $\theta = 0$ has been calculated exactly in Ref. [26]. This gap diminishes as θ increases as shown in Refs. [20,27] until reaching zero at $\theta = \pi$ if (1) holds.

III. MONTE CARLO PROGRAM

We have regularized the model (2) on a square lattice with periodic boundary conditions by the expression

$$S_L = A_L - i\theta Q_L, \quad A_L \equiv -\frac{1}{g_L} \sum_{x,\mu} \vec{\phi}(x) \cdot \vec{\phi}(x + \hat{\mu}), \tag{3}$$

where $Q_L = \sum_x Q_L(x)$ is the total lattice topological charge, $Q_L(x)$ the lattice topological charge density, and g_L the bare lattice coupling constant. The standard action A_L used in Eq. (3) is the simplest one on the lattice that reproduces A in Eq. (2) in the continuum limit.

The topological charge density has been regularized by defining it on triangles (not on single sites). Every plaquette of a square lattice can be cut through a diagonal into two triangles. If we call $\vec{\phi}_1$, $\vec{\phi}_2$, and $\vec{\phi}_3$ the fields at the sites of the three vertices (numbered counterclockwise) of one of these triangles, then the fraction of spherical angle subtended by these fields is $Q_L(\triangle)$ which satisfies (see Ref. [28])

$$\exp(2\pi i Q_L(\triangle)) = \frac{1}{\rho}(1 + \vec{\phi}_1 \cdot \vec{\phi}_2 + \vec{\phi}_2 \cdot \vec{\phi}_3 + \vec{\phi}_3 \cdot \vec{\phi}_1$$
$$+ i\vec{\phi}_1 \cdot (\vec{\phi}_2 \times \vec{\phi}_3)), \tag{4}$$

where $\rho^2 \equiv 2(1 + \vec{\phi}_1 \cdot \vec{\phi}_2)(1 + \vec{\phi}_2 \cdot \vec{\phi}_3)(1 + \vec{\phi}_3 \cdot \vec{\phi}_1)$ and $Q_L(\triangle) \in [-\frac{1}{2}, +\frac{1}{2}]$. Elementary plaquettes can be cut in two ways, but both choices lead to the same physical results for expectation values. The sum of $Q_L(\triangle)$ over all of the

triangles yields the so-called geometric topological charge Q_L, which provides integer values without requiring a composite operator renormalization.

A configuration of spins is a set of values of $\vec{\phi}(x)$ for all lattice points x that yields a definite number if plugged into expression (3).[3] Monte Carlo simulations permit one to collect configurations that are distributed according to the Boltzmann weight $\exp(-S_L)$ as long as S_L is real. Unfortunately, this condition fails to hold in our problem for $\theta \neq 0$. Indeed, the sign problem in the second term of S_L is evident due to the presence of the imaginary unit. The existence of this problem makes the model even more appealing since similar difficulties appear also in the lattice regularization of several field theories like QCD at finite baryon density. To avoid it, we have numerically simulated the action (3) at imaginary values of $\theta = -i\vartheta$ (ϑ is real) and extrapolated the results to real θ. Simulations were done using a Metropolis algorithm.

The simulations were all performed at $1/g_L = 1.6$ on a square lattice of lateral size $L = 180$. These choices were dictated by the need of working within a scaling window with as little finite-size and coarse-graining effects as possible. Specifically, as shown in Ref. [29], the size $L = 180$ is the one for which the model at $1/g_L = 1.6$ and $\theta = 0$ displays a ratio $L/\xi \sim 10$ (ξ is the correlation length or inverse of the gap). We will see later that, whereas ξ increases with θ, it decreases for increasing $|\vartheta|$. For this reason the ratio L/ξ becomes larger at nonzero ϑ and this fact enables us to maintain a good control on the finite-size effects in every single simulation. All these features were verified by explicit simulations on smaller lattice sizes ($L = 100$ and $L = 60$) obtaining numerically the same results within errors.

For the subsequent analysis, measurements of the topological charge and of the mass gap are needed. Measurements of the first observable are obtained by the procedure explained in the text around (4) and can be read off during the very Metropolis steps. To determine the mass gap (the inverse of the correlation length) we computed the two-point correlation function,

$$G(x_1, x_2) \equiv \langle \vec{\phi}(0,0) \cdot \vec{\phi}(x_1, x_2) \rangle, \tag{5}$$

where brackets $\langle \cdots \rangle$ indicate the average with the Boltzmann weight and x_1 and x_2 are the two components of x. The precise definition of correlation length we employed was

$$\xi \equiv \frac{\sqrt{\chi/\mathcal{F} - 1}}{2 \sin \pi/L}, \tag{6}$$

where χ is the magnetic susceptibility and $\mathcal{F}$ the correlation function at the smallest nonzero lattice momentum $2\pi/L$,

$$\chi \equiv \sum_{x_1, x_2} G(x_1, x_2),$$

$$\mathcal{F} \equiv \frac{1}{2} \sum_{x_1, x_2} (e^{2\pi i x_1/L} + e^{2\pi i x_2/L}) G(x_1, x_2). \tag{7}$$

---

[3]This definition excludes the so-called exceptional configurations, to which a value of the topological charge cannot be assigned unambiguously, but which constitute a set of zero measure [28].
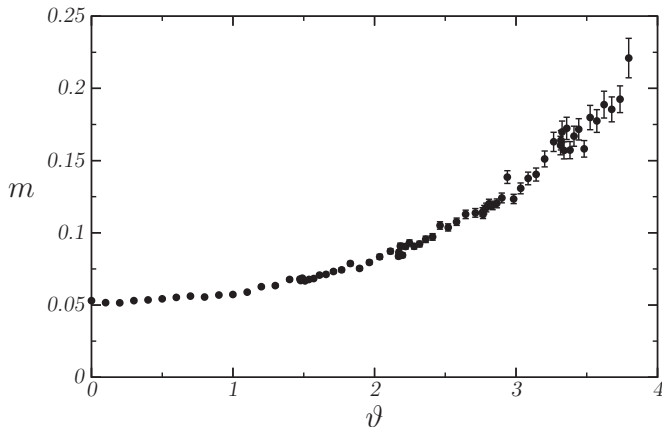
FIG. 1. Mass gap m, or inverse correlation length, as a function of $\vartheta = i\theta$ for $1/g_L = 1.6$.

Definition (6) has two advantages. On the one hand, the gap follows from a more straightforward calculation than the one employed in definitions based on the exponential decay of $G(x_1, x_2)$ (thus simplifying the error evaluation) and, on the other hand, the dependence of ξ on the lattice size L is as negligible as it is for the above-mentioned exponential decay-based definitions; see Ref. [30] (thus offering a very robust estimate). Errors were assessed by blocking.

We simulated the model for 75 different values of ϑ spanning from 0 to 3.7964. For each value of ϑ, two million of thermalized configurations were prepared. Each configuration and the next one were separated by 100 decorrelation hits and the norms of the fields ($\|\vec{\phi}(x)\| = 1$ for all x) were checked and reset every 20 Metropolis hits (actually, the whole procedure turned out to be numerically very stable since the residuals $\|\vec{\phi}\| - 1$ always remained negligibly small and in any case well within the computer accuracy). The Marsaglia random number generator was utilized.

The numerical results for the mass gap $m = 1/\xi$ and the average topological charge are shown in Figs. 1 and 2, as functions of $\vartheta = i\theta$. Since we want to investigate the behavior at real $\theta \simeq \pi$, we need to perform the analytic continuation of
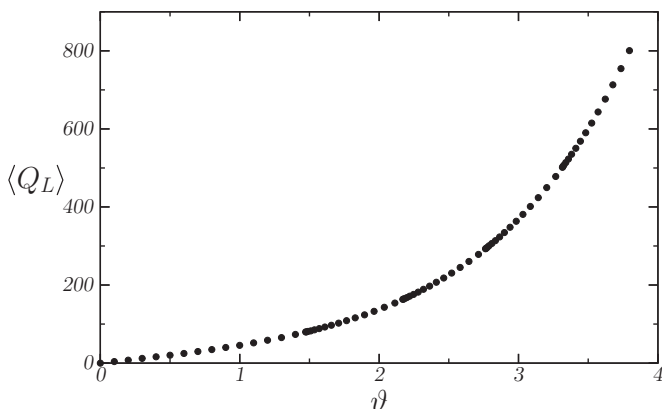

FIG. 2. Expectation value of the total topological charge, $\langle Q_L \rangle$, as a function of $\vartheta = i\theta$ for $1/g_L = 1.6$. Error bars are smaller than the size of the symbols.

our numerical data, which is known to be a difficult problem. This issue is discussed in the next section.

IV. METHOD OF SCALING TRANSFORMATIONS

The basic technique we want to use in order to understand the critical behavior at $\theta = \pi$ is that of scaling transformations proposed in Ref. [31] and subsequently used in Refs. [17,18,32,33]. This technique provides a controllable way to perform the analytic continuation of results obtained simulating at imaginary θ. We give here a brief description of this approach; more details can be found in the above-mentioned references.

Originally, the approach was proposed in order to study the behavior of the expectation value of the topological charge for systems with a θ term near $\theta = \pi$. Instead of working with the topological charge itself, it turns out to be more convenient to use the quantity

$$y(z) = \frac{\langle Q_L \rangle}{V \tanh \frac{\vartheta}{2}} \equiv \frac{q_\vartheta}{\tanh \frac{\vartheta}{2}}, \quad z = \cosh \frac{\vartheta}{2}, \quad z \geqslant 1, \quad (8)$$

where q_ϑ denotes the vacuum expectation value of Q_L over the volume V for imaginary $\theta = -i\vartheta$, making explicit by means of a subscript its dependence on ϑ for future convenience. Upon analytic continuation back to real values, $\vartheta \to i\theta$, one has

$$y(z) = -i \frac{q_{i\theta}}{\tan \frac{\theta}{2}}, \quad z = \cos \frac{\theta}{2}, \quad z \leqslant 1, \quad (9)$$

i.e., in terms of z the analytic continuation is simply an extrapolation from $z \geqslant 1$ to $z \leqslant 1$.[4] The next step consists in performing this extrapolation not by using directly $y(z)$ as a function of z, but rather by relating $y(z)$ to $y_\lambda(z) \equiv y(e^{\frac{\lambda}{2}} z)$, i.e., by trying to determine the function $y_\lambda(y)$. The assumption usually made is that $y(z)$ is a monotonically increasing function of z, and that moreover it vanishes only for $z = 0$ (i.e., $\theta = \pi$), which in physical terms corresponds to the absence of phase transitions sending the topological charge to zero in the interval $\theta \in (0,\pi)$. Actually, this is indeed the case for the models where the exact solution is known. The quantity y_λ is then a monotonic function $y_\lambda(y)$ of y, with the property that $y_\lambda = 0$ at $y = 0$. The expectation is that $y_\lambda(y)$ is a smooth function, so that starting from the smallest values of y that can be obtained by numerical simulations at real ϑ, one can reliably extrapolate towards $y = y_\lambda = 0$, i.e., in the region corresponding to real $\theta = -i\vartheta$. From this point of view, for asymptotically free systems the situation gets more and more favorable as one gets closer to the continuum limit, since topological fluctuations become suppressed.

In the 2D O(3) nonlinear sigma model, the behavior of the total topological charge near $\theta = \pi$ is related to that of the mass gap.[5] According to Haldane's conjecture, the mass gap vanishes as $m(\theta) \sim (\pi - \theta)^\epsilon \sim z^\epsilon$ (up to logarithmic

---

[4]Notice that $y(z)$ remains real also for $z \leqslant 1$.

[5]The well known problems that appear when taking the continuum limit of topological observables are not relevant for the problem at hand; see the discussion in Ref. [18] based on the results of Refs. [34,35].

corrections) for $\theta \to \pi$ from below, see Eq. (1), and since $q_{i\theta} \propto \partial m^2/\partial\theta$, one expects $y \sim (\pi - \theta)^{2\epsilon} \sim z^{2\epsilon}$. One can then determine the critical exponent ϵ of the mass gap by extrapolating the following effective exponent,

$$2\epsilon_q(y) \equiv \frac{2}{\lambda} \log \frac{y_\lambda(y)}{y}, \tag{10}$$

towards $y = 0$, i.e., towards $\theta = \pi$. One easily sees that $\epsilon_q(0) = \epsilon$. In principle, the same kind of technique can be used to study the behavior of any observable near $\theta = \pi$, and in particular one can work directly with the mass gap. Defining $m_\lambda(z) = m(e^{\frac{\lambda}{2}}z)$, reexpressing it as $m_\lambda(y)$, and defining the effective exponent

$$\epsilon_m(y) \equiv \frac{2}{\lambda} \log \frac{m_\lambda(y)}{m(y)}, \tag{11}$$

one finds again that $\epsilon_m(0) = \epsilon$.[6]

Despite the successful application of the method described above to several models [31–33], it turns out that the direct application of Eqs. (10) and (11) to the analysis of numerical data in the 2D O(3) nonlinear sigma model is hampered by the presence of logarithmic corrections to the critical behavior shown in Eq. (1); see Ref. [18]. In the next section we briefly discuss the form of these logarithmic corrections, and in Sec. VI we propose a method to overcome the related difficulties.

V. CRITICAL BEHAVIOR OF THE 2D O(3) NONLINEAR SIGMA MODEL WITH A TOPOLOGICAL TERM

The appropriate WZNW model describing the critical behavior of the 2D O(3) nonlinear sigma model with topological term near $\theta = \pi$ has been studied in Refs. [19,20,27]. In particular, in Ref. [20] the authors have determined the relation between the correlation length ξ and the coupling $\tilde{g} \sim \pi - \theta$ of the relevant perturbation near $\theta = \pi$, which reads

$$\frac{1}{\tilde{g}} \propto \xi^{\frac{3}{2}}(\log \xi)^{-\frac{3}{4}}[1 + \mathcal{O}(1/\log\xi)]. \tag{12}$$

Instead of working out the corresponding prediction for the critical behavior of the correlation length, we will use the more general expression

$$\frac{1}{\tilde{g}} = K\xi^a(\log \xi)^{-b}u(\log \xi), \tag{13}$$

with K some constant and some function $u(x) = 1 + \sum_{k=1}^{\infty} u_k x^{-k}$, which reduces to the results of Ref. [20] for $a = \frac{3}{2}$ and $b = \frac{3}{4}$ (and with an appropriate u). The reason why we do the calculation in this generalized setting is that we want a general expression for a vanishing mass gap, not relying on the details of the relevant critical model, which can be guessed on general grounds, and which can be used in principle to determine the critical exponents from numerical data, without knowing in advance the values of a and b. This is different from the approach of Refs. [13–15] where the theoretical expectation for the critical behavior was used as an input

of the numerical analysis. Since the theoretical prediction is strictly valid only in the continuum limit, a shortcoming of this approach is that it cannot be used to map the full phase diagram of the O(3) nonlinear sigma model at $\theta = \pi$ as the coupling is varied.[7] On the other hand, our approach is sufficiently general and could be applied to the study of this problem.

We now derive the critical behavior of the correlation length. Equation (13) can be inverted by solving for ξ iteratively. The solution has the form

$$\log \xi = \frac{1}{a} \log \frac{1}{\tilde{g}K} + \frac{b}{a} \log \log \frac{1}{\tilde{g}K} + \frac{b}{a} \log \frac{1}{a}$$
$$+ \sum_{l=1}^{\infty} \sum_{j=0}^{l} C_l^j \frac{\left(\log \log \frac{1}{\tilde{g}K}\right)^j}{\left(\log \frac{1}{\tilde{g}K}\right)^l}, \tag{14}$$

where C_l^j are constants. For our purposes we shall use the variable $z = \cos\frac{\theta}{2}$, which behaves as $z \simeq (\pi - \theta)/2$ near π and is therefore proportional to $\tilde{g}$. Subleading terms in the expansion of z are powers in $\tilde{g}$ (and vice versa) and so will be discarded, since we are considering here only logarithmic terms, which dominate the critical behavior. We obtain

$$\log \xi \overset{P}{=} \frac{1}{a} \log \frac{1}{z} + \frac{b}{a} \log \log \frac{1}{z} + \bar{C}_0^0$$
$$+ \sum_{l=1}^{\infty} \sum_{j=0}^{l} \bar{C}_l^j \frac{\left(\log \log \frac{1}{z}\right)^j}{\left(\log \frac{1}{z}\right)^l}, \tag{15}$$

where the mark P over the equals sign indicates that the equality holds up to terms which are proportional to powers of z, and $\bar{C}_l^j$ are constants. Recalling now that the mass gap is $m = 1/\xi$, and exponentiating Eq. (15), we finally get

$$m \overset{P}{=} z^\epsilon \left(\log \frac{1}{z}\right)^{-\beta} \exp\left\{-\sum_{l=0}^{\infty} \sum_{j=0}^{l} \bar{C}_l^j \frac{\left(\log \log \frac{1}{z}\right)^j}{\left(\log \frac{1}{z}\right)^l}\right\}, \tag{16}$$

where $\epsilon = \frac{1}{a}$ and $\beta = \frac{b}{a}$. Substituting the values appearing in Eq. (12), one obtains the theoretical expectation for the critical exponents, $\epsilon_{\text{WZNW}} = \frac{2}{3}$ and $\beta_{\text{WZNW}} = \frac{1}{2}$.

Even though most of the coefficients in Eq. (16) are not fully determined, as the detailed form of the function u in Eq. (13) is largely unknown, nevertheless the coefficients $\bar{C}_l^l = C_l^l, l \geqslant 1$ can be determined exactly, as they do not depend on u, and the corresponding terms can be resummed. Setting $w = \log\frac{1}{z}$, $m_0 = e^{-\bar{C}_0^0}$, and

$$\bar{u}(w) = \exp\left\{-\sum_{l=1}^{\infty} \sum_{j=0}^{l-1} \bar{C}_l^j \frac{(\log w)^j}{w^l}\right\} = 1 + \mathcal{O}(1/w), \tag{17}$$

we finally obtain

$$m \overset{P}{=} m_0 e^{-\epsilon w} w^{-\beta} \left[1 + \frac{\beta}{\epsilon} \frac{\log w}{w}\right]^{-\beta} \bar{u}(w). \tag{18}$$

The critical behavior of the expectation value of the topological charge density, $q_{i\theta}$, can be obtained from that of the mass

---

[6]We assume here that there are no phase transitions for $\theta \in (0,\pi)$ that send the mass to zero.

[7]For example, at strong coupling the system is expected to undergo a first-order phase transition at $\theta = \pi$.

gap m. Since according to the usual renormalization-group arguments the free energy per unit volume F is proportional to m^2, one has $q_{i\theta} = -i\partial F/\partial\theta \overset{P}{\propto} m\,\partial m/\partial\theta \overset{P}{\propto} m\,\partial m/\partial z$. More precisely, writing $m = m_0 e^{-\epsilon w} w^{-\beta} f(w)$, with $f(w) = 1 + \mathcal{O}(\log w/w)$, we have for y [see Eqs. (8) and (9)]

$$y \overset{P}{=} z q_{i\theta} \overset{P}{\propto} m z \frac{\partial m}{\partial z} = -m\frac{\partial m}{\partial w} \overset{P}{=} m^2\left(\epsilon + \frac{\beta}{w} - \frac{\tilde{f}(w)}{w}\right),$$

(19)

where $\tilde{f}(w) = w f'(w)/f(w) = \mathcal{O}(\log w/w)$. We can therefore write

$$y \overset{P}{=} y_0 e^{-2\epsilon w} w^{-2\beta}\left[1 + \frac{\beta}{\epsilon}\frac{\log w}{w}\right]^{-2\beta} \bar{v}(w),$$

(20)

with some constant y_0, and with $\bar{v}(w) = 1 + \mathcal{O}(1/w)$. It is now straightforward to derive expressions for the effective exponents. They read

$$\epsilon_m(y) = \frac{2}{\lambda}\log\frac{m_\lambda}{m}$$

$$\overset{P}{=} \epsilon\left(1 + \frac{\beta}{\epsilon}\frac{1}{w} - \frac{\beta^2}{\epsilon^2}\frac{\log w}{w^2 + \frac{\beta}{\epsilon}w\log w}\right) + \mathcal{O}(1/w^2)$$

$$= \epsilon\left(1 + \frac{\beta}{\epsilon}\frac{1}{w + \frac{\beta}{\epsilon}\log w}\right) + \mathcal{O}(1/w^2),$$

(21)

$$2\epsilon_q(y) = \frac{2}{\lambda}\log\frac{y_\lambda}{y}$$

$$\overset{P}{=} 2\epsilon\left(1 + \frac{\beta}{\epsilon}\frac{1}{w} - \frac{\beta^2}{\epsilon^2}\frac{\log w}{w^2 + \frac{\beta}{\epsilon}w\log w}\right) + \mathcal{O}(1/w^2)$$

$$= 2\epsilon\left(1 + \frac{\beta}{\epsilon}\frac{1}{w + \frac{\beta}{\epsilon}\log w}\right) + \mathcal{O}(1/w^2),$$

(22)

where w has to be traded for y by inverting the following relation:

$$\frac{1}{2\epsilon}\log\frac{y_0}{y} = w + \frac{\beta}{\epsilon}\log w + \mathcal{O}(\log w/w).$$

(23)

VI. DETERMINATION OF THE CRITICAL EXPONENTS

The presence of the logarithmic factors $w^{-\beta}$ and $w^{-2\beta}$ in Eqs. (18) and (20) constitutes a problem for the numerical analysis. It is well known that the presence of logarithmic corrections can lead to a wrong estimate of a critical exponent. In the problem at hand, the main consequences of these corrections are the $\mathcal{O}(1/w) = \mathcal{O}(1/\log\frac{y_0}{y})$ terms in Eqs. (21) and (22), which lead to rather large deviations from the value at $y = 0$ even for pretty small y. Furthermore, the $\mathcal{O}(\log w/w)$ term in Eq. (23) results into $\mathcal{O}(\log\log\frac{y_0}{y}/(\log\frac{y_0}{y})^2)$ terms in Eqs. (21) and (22), that also give sizable contributions. On top of that, the $\log w$ term in Eq. (23) spoils the approximate linearity of the relation between $\log\frac{y_0}{y}$ and w at small w. As a consequence, these terms make it very difficult to correctly identify the asymptotic value as $y \to 0$.

To overcome this problem, it is therefore convenient to first remove the logarithmic factor, and only after perform the analysis with the scaling transformations, as suggested in Ref. [18]. An obvious obstacle is that in principle we

do not know the exponent β. In Ref. [18] the analysis was performed by taking $\beta = \frac{1}{2}$, in accordance with the theoretical expectation, and trying to determine the critical exponent by fitting the data for the properly modified effective exponent obtained from the topological charge. The results were in agreement with the theoretical expectation. Here we use another strategy that does not presume any preferred value for β: by choosing an arbitrary β, we obtain two determinations of the critical exponent by fitting separately the data for two properly defined effective exponents, involving respectively the mass gap and the topological charge, as if the current value of β were the correct one. We then vary β, obtaining two sets of putative critical exponents, one for each observable. The idea is that for the correct choice of β, the two determinations have to coincide.

To determine the mass gap critical exponent from the mass gap data, it is therefore convenient to study the behavior of the quantity $\bar{m} = m(\log\frac{1}{z})^\beta = mw^\beta$ under the rescaling $z \to e^{\frac{\lambda}{2}}z$, or equivalently under the shift $w \to w - \frac{\lambda}{2}$. Analogously, to determine the mass gap critical exponent from the topological charge data it is convenient to consider $\bar{y} = y(\log\frac{1}{z})^{2\beta} = yw^{2\beta}$. To lowest order[8] we find from Eqs. (21) and (22)

$$\frac{2}{\lambda}\log\frac{\bar{m}_\lambda}{\bar{m}} \overset{P}{=} \epsilon\left(1 - \frac{\beta^2}{\epsilon^2}\frac{\log w}{w^2 + \frac{\beta}{\epsilon}w\log w}\right) + \mathcal{O}(1/w^2), \quad (24)$$

$$\frac{2}{\lambda}\log\frac{\bar{y}_\lambda}{\bar{y}} \overset{P}{=} 2\epsilon\left(1 - \frac{\beta^2}{\epsilon^2}\frac{\log w}{w^2 + \frac{\beta}{\epsilon}w\log w}\right) + \mathcal{O}(1/w^2). \quad (25)$$

Finally, since to lowest order[9] $w = \log(1/z) = (1/2\epsilon)\log(y_0/\bar{y}) + o(1)$, one can write down the relation between the effective exponents and $\bar{y}$.

A possible practical definition of $\bar{m}$ and $\bar{y}$ is (recall that $z = \cosh\frac{\vartheta}{2}$)

$$\bar{m} \equiv m\ell^\beta, \quad \bar{y} \equiv y\ell^{2\beta}, \quad \ell = \log\left(1 + \frac{1}{z}\right). \quad (26)$$

However, to avoid distortions at large ϑ which could worsen the quality of the numerical analysis, it is preferable to work instead with the quantities

$$\tilde{m} \equiv m\left(\frac{\ell z}{\log 2}\right)^\beta, \quad \tilde{y} \equiv y\left(\frac{\ell z}{\log 2}\right)^{2\beta}, \quad (27)$$

where we have also introduced a factor $\log 2$ to give 1 in front of m and y at $\vartheta = 0$. These quantities are easily seen to satisfy

$$\frac{2}{\lambda}\log\frac{\tilde{m}_\lambda}{\tilde{m}} - \beta \overset{P}{=} \epsilon\left(1 - \frac{\beta^2}{\epsilon^2}\frac{\log w}{w^2 + \frac{\beta}{\epsilon}w\log w}\right) + \mathcal{O}(1/w^2),$$

(28)

$$\frac{2}{\lambda}\log\frac{\tilde{y}_\lambda}{\tilde{y}} - 2\beta \overset{P}{=} 2\epsilon\left(1 - \frac{\beta^2}{\epsilon^2}\frac{\log w}{w^2 + \frac{\beta}{\epsilon}w\log w}\right) + \mathcal{O}(1/w^2).$$

(29)

---

[8] Due to the resummation done in Eq. (18), Eqs. (24) and (25) actually contain higher-order terms.

[9] Notice the absence of $\mathcal{O}(\log\log(y_0/\bar{y}))$ corrections, which are present in the relation between $\log(y_0/y)$ and w; see Eq. (23).

For our purposes it is convenient to reexpress the quantities on the left-hand side of Eqs. (28) and (29) as functions of $\tilde{y}$. A simple calculation shows that

$$\log \frac{\tilde{y}_0}{\tilde{y}} = 2(\epsilon + \beta)w + \mathcal{O}(\log w/w), \qquad (30)$$

where $\tilde{y}_0 = y_0/(\log 2)^{2\beta}$, which allows one to recast Eqs. (28) and (29) as

$$\tilde{\epsilon}_m(\tilde{y}) \equiv \frac{2}{\lambda} \log \frac{\tilde{m}_\lambda}{\tilde{m}} - \beta$$

$$\stackrel{P}{=} \epsilon \, \mathcal{E}\left(\frac{1}{2(\epsilon + \beta)} \log \frac{\tilde{y}_0}{\tilde{y}}\right) + \mathcal{O}\left(\left(\log \frac{\tilde{y}_0}{\tilde{y}}\right)^{-2}\right), \quad (31)$$

$$2\tilde{\epsilon}_q(\tilde{y}) \equiv \frac{2}{\lambda} \log \frac{\tilde{y}_\lambda}{\tilde{y}} - 2\beta$$

$$\stackrel{P}{=} 2\epsilon \, \mathcal{E}\left(\frac{1}{2(\epsilon + \beta)} \log \frac{\tilde{y}_0}{\tilde{y}}\right) + \mathcal{O}\left(\left(\log \frac{\tilde{y}_0}{\tilde{y}}\right)^{-2}\right), \quad (32)$$

where

$$\mathcal{E}(x) = 1 - \frac{\beta^2}{\epsilon^2} \frac{\log x}{x^2 + \frac{\beta}{\epsilon} x \, \log x}. \qquad (33)$$

These expressions can be used to fit the numerical data for small enough $\tilde{y}$. Since these are low-order approximations to the exact expressions, one is introducing a systematic error through the truncation. We remind the reader that by "exact" we mean here up to terms originating from powers of z in Eq. (15), which should be negligible compared to the logarithmic terms. We mention here that the values of ϑ at which we performed the simulations were chosen in such a way that corresponding pairs of z and $e^{\frac{\lambda}{2}} z$ could be constructed with $\lambda = 0.5$, so that we did not need any interpolation to compute $\tilde{\epsilon}_m$ and $\tilde{\epsilon}_q$.

A practical way to estimate the systematic error due to truncation on our determinations of the critical exponent is to employ the technique of constrained fits [36]. This basically consists in adding more and more subleading corrections to Eqs. (31) and (32), constraining the corresponding coefficients according to the available information. When the error on the parameters given by the fitter settles against the increase of the number of terms, it includes also the contribution of the systematic error due to the truncation of the exact expression [36]. One can show that by including higher-order terms, Eqs. (31) and (32) become[10]

$$\tilde{\epsilon}_m \stackrel{P}{=} \epsilon \, \mathcal{E}(\Lambda) + \sum_{k=2}^{\infty} \sum_{j=0}^{k-2} h_{jk}^{(m)} \frac{(\log \Lambda)^j}{\Lambda^k}, \qquad (34)$$

$$2\tilde{\epsilon}_q \stackrel{P}{=} 2\epsilon \, \mathcal{E}(\Lambda) + \sum_{k=2}^{\infty} \sum_{j=0}^{k-2} h_{jk}^{(q)} \frac{(\log \Lambda)^j}{\Lambda^k}, \qquad (35)$$

---

[10]Notice that similar expansions for ϵ_m and ϵ_q as functions of $\Lambda_0 = \frac{1}{2\epsilon} \log \frac{y_0}{y}$ contain, besides a $1/\Lambda_0$ term, also terms proportional to $(\log \Lambda_0)^j/\Lambda_0^{j+1}$, which are absent in $\tilde{\epsilon}_m$ and $\tilde{\epsilon}_q$.

TABLE I. Priors used in the constrained fits for $\tilde{\epsilon}_q(\tilde{y})$.

Parameter	Mean	Standard deviation
ϵ	1	100
$\tilde{y}_0$	1.0	1.0
$h_{02}^{(q)}$	0.1	0.1
$h_{13}^{(q)}$	−0.1	0.1
$h_{03}^{(q)}$	0.1	0.1
$h_{24}^{(q)}$	0.0	0.1
$h_{14}^{(q)}$	0.0	0.01
$h_{04}^{(q)}$	0.0	0.01

where we set $\Lambda \equiv \frac{1}{2(\epsilon + \beta)} \log \frac{\tilde{y}_0}{\tilde{y}}$. The constraints on the parameters ("priors") are needed to ensure the stability of fits with a rather large number of parameters. The priors were chosen to be as loose as possible while leading to fits of good quality.

We have applied this technique to the critical exponent measured from the expectation value of the topological charge. In practice we assumed that the fit parameters obey a Gaussian distribution, with mean and standard deviation as reported in Table I. We used data up to $\tilde{y} = 0.01$, and up to eight fit parameters. The results of the fit are shown in Fig. 3.

The same kind of analysis should be performed for the critical exponent obtained from the mass gap, i.e., one should fix $\tilde{y}_0$ to the value obtained using the total topological charge data, and fit the mass gap data including more and more terms in the expansion to determine the systematic error. However, the quality of the data for $\tilde{\epsilon}_m$ is rather poor compared to the very precise topological charge data, and very hard to improve (we remind the reader that we made two million measurements for each ϑ). The mass gap data show no clear structure, being essentially constant within the statistical errors; see Fig. 4. An attempt at including the main contribution and the first subleading term in Eq. (34) results in fits that are very sensitive to the choice of priors, indicating that the data are not good enough for a sophisticated analysis like the one carried out for the topological charge. However, if the absence of a clear structure in the data for $\tilde{\epsilon}_m$ indicates that the size of the corrections to the value at $\tilde{y} = 0$ is of the same order of the
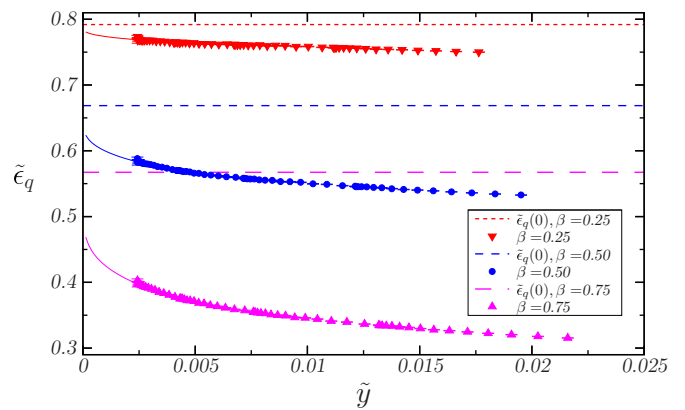

FIG. 3. (Color online) Data (points), fit (solid line), and value at $\tilde{y} = 0$ (dashed line) for the effective exponent $\tilde{\epsilon}_q$, for three assumed values of β.
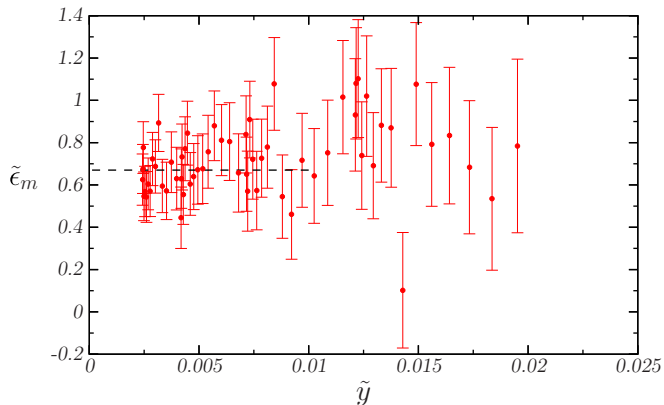
FIG. 4. (Color online) Data for the effective exponent $\tilde{\epsilon}_m$ (points) and result of a fit with a constant (dashed line), assuming $\beta = 0.5$.
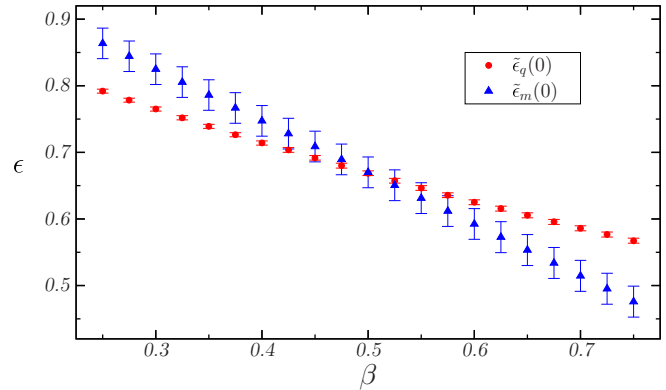

FIG. 5. (Color online) The two determinations $\tilde{\epsilon}_q(0)$ and $\tilde{\epsilon}_m(0)$ of the mass gap critical exponent ϵ, as a function of the assumed value of β.

statistical errors, then a fit to the data with a simple constant will result into a reasonable estimate of the critical exponent, and the statistical fluctuations around the central value will give a reasonable estimate of the error. We shall follow this latter strategy to determine the critical exponent of the mass gap.

The results for the two determinations of the critical exponent are reported in Table II. In Fig. 5 we compare the two determinations, which clearly cross close to $\beta = 0.5$. We take this value for β, and for the corresponding error we take

TABLE II. Results for $\tilde{\epsilon}_q(0)$, obtained with a eight-parameter constrained fit of $\tilde{\epsilon}_q$, and results for $\tilde{\epsilon}_m(0)$ obtained with a fit of $\tilde{\epsilon}_m$ with a constant, for several assumed values of β.

β	$\tilde{\epsilon}_q(0)$	$\tilde{\epsilon}_m(0)$
0.250	$0.7919^{+0.0028}_{-0.0030}$	0.864 ± 0.023
0.275	$0.7784^{+0.0029}_{-0.0030}$	0.844 ± 0.023
0.300	$0.7651^{+0.0030}_{-0.0031}$	0.825 ± 0.023
0.325	$0.7520^{+0.0030}_{-0.0031}$	0.805 ± 0.023
0.350	$0.7391^{+0.0031}_{-0.0032}$	0.786 ± 0.023
0.375	$0.7264^{+0.0031}_{-0.0032}$	0.767 ± 0.023
0.400	$0.7140^{+0.0031}_{-0.0032}$	0.747 ± 0.023
0.425	$0.7037^{+0.0035}_{-0.0036}$	0.728 ± 0.023
0.450	$0.6918^{+0.0035}_{-0.0036}$	0.709 ± 0.023
0.475	$0.6801^{+0.0035}_{-0.0036}$	0.689 ± 0.023
0.500	$0.6687^{+0.0035}_{-0.0036}$	0.670 ± 0.023
0.525	$0.6574^{+0.0035}_{-0.0036}$	0.651 ± 0.023
0.550	$0.6464^{+0.0035}_{-0.0036}$	0.631 ± 0.023
0.575	$0.6357^{+0.0035}_{-0.0036}$	0.612 ± 0.023
0.600	$0.6251^{+0.0035}_{-0.0036}$	0.592 ± 0.023
0.625	$0.6156^{+0.0037}_{-0.0037}$	0.573 ± 0.023
0.650	$0.6055^{+0.0037}_{-0.0037}$	0.553 ± 0.023
0.675	$0.5957^{+0.0037}_{-0.0038}$	0.534 ± 0.023
0.700	$0.5860^{+0.0037}_{-0.0038}$	0.515 ± 0.023
0.725	$0.5766^{+0.0038}_{-0.0038}$	0.495 ± 0.023
0.750	$0.5674^{+0.0038}_{-0.0038}$	0.476 ± 0.023

the half-length of the interval $[0.425, 0.575]$, where the two determinations are compatible within one standard deviation, which results in $\beta = 0.50(7)$. For the critical exponent, we take the average of the values of $\tilde{\epsilon}_m(0)$ and $\tilde{\epsilon}_q(0)$ at $\beta = 0.5$, and we quote as error the half-variation of $\tilde{\epsilon}_m(0)$ in the range $\beta \in [0.425, 0.575]$, which yields $\epsilon = 0.67(6)$. These values are in very good agreement with the theoretical expectation $\epsilon_{\mathrm{WZNW}} = \frac{2}{3}$ and $\beta_{\mathrm{WZNW}} = \frac{1}{2}$ for the critical exponent and the exponent of the logarithmic correction. For completeness, we finish by noting that had we established the value of $\beta = 1/2$ from the very beginning, as in Ref. [18], then the determination of ϵ obtained from the topological charge would have read $\tilde{\epsilon}_q(0) = 0.6687^{+0.0035}_{-0.0036}$.

VII. CONCLUSIONS

The present paper deals with Haldane's conjecture, which states that the mass gap in the 2D O(3) nonlinear sigma model with a θ term must vanish as θ approaches the value π according to the precise law given in Eq. (1). The aim of the work is to extract the critical exponent ϵ ruling the dominant, power-law behavior of the mass gap near $\theta = \pi$ and also the elusive exponent β of its logarithmic correction, without any *a priori* assumption about their values.

The sign problem hindering the numerical study of the model in the presence of a nonzero θ has been circumvented by performing Monte Carlo simulations at imaginary values of θ (where the Euclidean action is real and a positive Boltzmann weight can be safely defined) and extrapolating the results to real values of θ.

The basic technique adopted to carry out this extrapolation is that of scaling transformations proposed in Ref. [31]. Had we limited our analysis to the mass gap only, the target would have been missed, even in spite of high-statistics Monte Carlo simulations, due to the intrinsically bad signal-to-noise ratio of this observable (this problem arose in Ref. [16]).

The breakthrough comes by the inclusion in the analysis of a second observable, the topological charge, for which very accurate determinations at imaginary θ can be obtained. Indeed, when the compatibility between the extrapolations towards $\theta = \pi$ of the mass gap and of the topological charge is imposed, a determination of both the exponents ϵ and β gets within reach, nicely agreeing with the theoretical prediction.

These determinations, schematically summarized in Fig. 5, are $\epsilon = 0.67(6)$ and $\beta = 0.50(7)$, both in concordance with the renormalization-group prediction of Refs. [19,20] shown in Eq. (1), namely $\epsilon_{\text{WZNW}} = \frac{2}{3}$ and $\beta_{\text{WZNW}} = \frac{1}{2}$.

ACKNOWLEDGMENTS

[1] F. D. M. Haldane, Phys. Lett. A **93**, 464 (1983).

[2] F. D. M. Haldane, Phys. Rev. Lett. **50**, 1153 (1983).

[3] F. D. M. Haldane, J. Appl. Phys. **57**, 3359 (1985).

[4] E. H. Lieb, T. Schultz, and D. Mattis, Ann. Phys. (NY) **16**, 407 (1961).

[5] R. Botet and R. Jullien, Phys. Rev. B **27**, 613(R) (1983); R. Botet, R. Jullien, and M. Kolb, *ibid.* **29**, 5222 (1984).

[6] I. Affleck and E. H. Lieb, Lett. Math. Phys. **12**, 57 (1986).

[7] I. Affleck, T. Kennedy, E. H. Lieb, and H. Tasaki, Phys. Rev. Lett. **59**, 799 (1987).

[8] I. Affleck, T. Kennedy, E. H. Lieb, and H. Tasaki, Commun. Math. Phys. **115**, 477 (1988).

[9] U. Schollwöck and T. Jolicoeur, Europhys. Lett. **30**, 493 (1995).

[10] I. Affleck, Phys. Rev. Lett. **66**, 2429 (1991).

[11] E. Fradkin, *Field Theories of Condensed Matter Systems* (Addison-Wesley, Redwood City, CA, 1991).

[12] C. Torrero, O. Borisenko, V. Kushnir, B. Allés, and A. Papa, PoS LATTICE **2013**, 338 (2013), arXiv:1311.4292.

[13] W. Bietenholz, A. Pochinsky, and U.-J. Wiese, Phys. Rev. Lett. **75**, 4524 (1995).

[14] M. Bögli, F. Niedermayer, M. Pepe, and U.-J. Wiese, J. High Energy Phys. 04 (2012) 117.

[15] P. de Forcrand, M. Pepe, and U.-J. Wiese, Phys. Rev. D **86**, 075006 (2012).

[16] B. Allés and A. Papa, Phys. Rev. D **77**, 056008 (2008).

[17] V. Azcoiti, G. Di Carlo, and A. Galante, Phys. Rev. Lett. **98**, 257203 (2007).

[18] V. Azcoiti, G. Di Carlo, E. Follana, and M. Giordano, Phys. Rev. D **86**, 096009 (2012).

[19] I. Affleck and F. D. M. Haldane, Phys. Rev. B **36**, 5291 (1987).

[20] I. Affleck, D. Gepner, H. J. Schulz, and T. Ziman, J. Phys. A: Math. Gen. **22**, 511 (1989).

[21] J. Wess and B. Zumino, Phys. Lett. B **37**, 95 (1971).

[22] S. P. Novikov, Sov. Math. Dokl. **24**, 222 (1981).

[23] E. Witten, Commun. Math. Phys. **92**, 455 (1984).

[24] A. M. M. Pruisken and I. S. Burmistrov, Ann. Phys. (NY) **316**, 285 (2005).

[25] A. A. Belavin and A. M. Polyakov, JETP Lett. **22**, 245 (1975).

[26] P. Hasenfratz, M. Maggiore, and F. Niedermayer, Phys. Lett. B **245**, 522 (1990).

[27] D. Controzzi and G. Mussardo, Phys. Rev. Lett. **92**, 021601 (2004).

[28] B. Berg and M. Lüscher, Nucl. Phys. B **190**, 412 (1981).

[29] B. Allés, G. Cella, M. Dilaver, and Y. Gündüç, Phys. Rev. D **59**, 067703 (1999).

[30] B. Allés, A. Buonanno, and G. Cella, Nucl. Phys. B **500**, 513 (1997).

[31] V. Azcoiti, G. Di Carlo, A. Galante, and V. Laliena, Phys. Lett. B **563**, 117 (2003).

[32] V. Azcoiti, G. Di Carlo, A. Galante, and V. Laliena, Phys. Rev. D **69**, 056006 (2004).

[33] V. Azcoiti, E. Follana, and A. Vaquero, Nucl. Phys. B **851**, 420 (2011).

[34] G. Bhanot, R. F. Dashen, N. Seiberg, and H. Levine, Phys. Rev. Lett. **53**, 519 (1984).

[35] D. Nógrádi, J. High Energy Phys. 05 (2012) 089.

[36] G. P. Lepage, B. Clark, C. T. H. Davies, K. Hornbostel, P. B. Mackenzie, C. Morningstar, and H. Trottier, Nucl. Phys. B, Proc. Suppl. **106**, 12 (2002).